Journal of Solid State Chemistry 182 (2009) 141–146

Contents lists available at ScienceDirect

Journal of Solid State Chemistry

journal homepage: www.elsevier.com/locate/jssc

Synthesis, structure and physicochemical characterization of a noncentrosymmetric, quaternary thiostannate: $EuCu_2SnS_4$

Jennifer A. Aitken *, Jonathan W. Lekse, Jin-Lei Yao, Rosalynn Quinones

Department of Chemistry and Biochemistry, Duquesne University, Pittsburgh, PA 15282, USA

ARTICLE INFO

Article history:
Received 13 June 2008
Received in revised form
18 September 2008
Accepted 21 September 2008
Available online 14 October 2008

Keywords:
Thiostannate
Europium
Chalcogenide
Synthesis
Lanthanide
Sulfide

ABSTRACT

$EuCu_2SnS_4$ was prepared by a stoichiometric combination of the elements heated to 700 °C for 125 h. The structure was determined by single crystal X-ray diffraction methods. The compound crystallizes in the noncentrosymmetric, orthorhombic space group *Ama*2 with $a = 10.4793(1)$ Å, $b = 10.3610(2)$ Å, $c = 6.4015(1)$ Å, $Z = 4$, $R1 = 0.99\%$ and $wR2 = 2.37\%$. The structure type is that of $SrCu_2GeSe_4$. The structure can be described as a three-dimensional network built from near perfect SnS_4 and distorted CuS_4 tetrahedra together with EuS_8 square antiprisms. The dark red compound is a semiconductor with an optical bandgap of 1.85 eV.

1. Introduction

Tin sulfides display a rich structural chemistry and possess attractive optical and electrical properties [1]. Europium chalcogenides are also very interesting from a structural standpoint and may possess technologically useful characteristics. For example, Eu_2GeS_4 and Eu_2GeSe_4 are promising ferroelectric materials with T_c values of 335 and 620 K, respectively [2]. Additionally, intriguing magnetic behavior has been observed for several europium-containing chalcogenides, such as metamagnetic transitions in $Eu_5Sn_3S_{12}$ [3] and $EuSe_2$ [4,5].

Europium, many times, can be found in the 2+ oxidation state in a chalcogenide environment, frequently resulting in the chemistry of europium-containing chalcogenides being different from those of the other lanthanide metals which would prefer the 3+ or 4+ oxidation states [4]. Additionally, mixed valent europium compounds can be obtained, sometimes with crystallographically unique positions for each oxidation state of europium, and sometimes with mixed valency on the same crystallographic sites. Several europium-containing chalcogenides have been previously reported such as KEu_2CuS_6 (Eu^{3+}) [6], $KEuGeS_4$ (Eu^{3+}) [7], $LiEuPSe_4$ (Eu^{2+}) [8], $Na_2EuGeSe_4$ (Eu^{2+}) [9], $Na_{0.75}Eu_{1.625}GeSe_4$ (Eu^{2+}) [9], $K_2EuGeSe_5$ (Eu^{2+}) [7], $Eu_3Sn_2S_7$ (Eu^{2+}) [10,11], Eu_2SnS_4 (Eu^{2+}) [11,12], Eu_2GeS_4 (Eu^{2+}) [2], $Eu_3Ge_3S_9$ (Eu^{2+}) [13], $Eu_4Sn_2S_9$ (Eu^{2+} and Eu^{3+}) [11] and $Eu_5Sn_3S_{12}$ (Eu^{2+} and Eu^{3+}) [3,11,14,15], as well as others. In cases where Eu is found in the 2+ oxidation state, similarities with alkaline-earth-containing analogs often occur.

Here we report the synthesis, structure and optical properties of $EuCu_2SnS_4$, as well as structural comparisons with related phases. Interestingly, the title compound, $EuCu_2SnS_4$, has also been prepared by Llanos and coworkers [16]; however, they reported that it is isostructural with $SrCu_2SnS_4$, $BaCu_2GeS_4$ and $SrCu_2GeS_4$, which are reported to crystallize in the space group $P3_1$ (No. 144) [17,18], while we report that $EuCu_2SnS_4$ crystallizes in the $SrCu_2GeSe_4$ structure-type [19] with the space group *Ama*2. A search of the literature revealed that several other related compounds crystallize in this same structure type or similar types, namely $BaCu_2SnSe_4$ [20], Sr_2SnS_4, γ-Sr_2GeSe_4 [12] and Li_2EuPSe_4 [8]. $EuCu_2SnS_4$ and these other compounds will be discussed collectively.

2. Experimental

2.1. Reagents

Chemicals in this work were used as obtained: (i) copper powder, −100 mesh, 99.999%, Strem; (ii) europium powder, −40 mesh, 99.9%, Cerac; (iii) tin powder, −100 mesh, 99.999%, Strem; (iv) sulfur sublimed powder, 99.5%, Fisher.

* Corresponding author. Fax: +1 412 396 5683.
E-mail address: aitkenj@duq.edu (J.A. Aitken).

0022-4596/$ - see front matter © 2008 Elsevier Inc. All rights reserved.
doi:10.1016/j.jssc.2008.09.022

2.2. Synthesis

2.2.1. Synthesis of $EuCu_2SnS_4$ microcrystalline powder

A 1 mmol sample of $EuCu_2SnS_4$ was synthesized from a stoichiometric mixture of the elements. The starting materials were ground for 15 min in an argon-filled glovebox and placed into a graphite crucible. The crucible was then sealed under a vacuum of 10^{-3} mbar in a 12 mm o.d. fused-silica tube. The tube was placed into a programmable furnace and heated to 700 °C in 12 h. The sample was held at this temperature for 125 h and then quenched in an ice-water bath. The tube was opened and the sample removed from the crucible. The product consisted of a dark red microcrystalline powder that was ground in preparation for characterization. The material is air-stable.

2.2.2. Synthesis of $EuCu_2SnS_4$ single crystals

The same procedure as that described above was used, with the exception of the heating profile. This reaction was heated to 800 °C in 12 h, held at 800 °C for 125 h, slow cooled to 500 °C in 50 h and then rapidly cooled to room temperature. The product consisted of dark red block-like crystals. A suitable single crystal was selected for single crystal X-ray diffraction studies. Although this reaction produced the best crystals, it had a larger amount of impurity/unwanted phases and was not used for other characterization.

2.3. Physical measurements

2.3.1. Powder X-ray diffraction (PXRD) and Reitveld refinement

Powder X-ray diffraction patterns were collected using a Panalytical X'Pert Pro MPD powder X-ray diffractometer operating at 45 kV and 40 mA and using copper $K\alpha$ radiation ($\lambda = 1.541871$ Å). Data were collected as a continuous scan from 10 to 100°2θ, with a step width of 0.08° and the time per step of 80 s. The divergence slit was fixed at 1/4° and the anti-scatter slit at 1/2°. Samples were prepared for analysis by grinding the sample powder for more than a half hour in an agate mortar and pestle and then back filling the material into the aluminum sample holder. Samples were spun during data collection.

The Rietveld refinement was carried out using GSAS with an interface of EXPGUI [21,22]. A Pseudo-Voigt function was used to model the peak profile and the background was described as a shifted Chebyschev type. The following parameters were refined: scale factor, background, peak profile shape, lattice parameters, atomic coordinates and isotropic displacement parameters (U_{iso}).

2.3.2. Scanning electron microscopy (SEM) and energy dispersive spectroscopy (EDS)

A CamScan Series 4 scanning electron microscope was used to image samples and a Princeton Gamma Tech detector was used for EDS. The working distance was 35 mm and the accelerating voltage was set to 22.5 kV. Samples were mounted onto double-sided carbon tape, which was adhered to an aluminum specimen holder. EDS data were collected for 60 s.

2.3.3. Single crystal X-ray diffraction

A dark, red rectangular crystal measuring $0.05 \times 0.08 \times 0.17$ mm^3 was mounted onto a glass fiber using Krazy® glue. Over a hemisphere of data was collected using 0.3° steps in omega with a Bruker SMART Apex II diffractometer at room temperature with a graphite monochomator, using a CCD detector and Mo $K\alpha$ radiation (0.71073 Å). 3369 reflections were observed of which 3189 were used after integration using SAINT [23] for the final cell refinement. An empirical absorption correction was performed using SADABS. The structure solution and full-matrix least-squares refinement on F^2 were performed using SHELXTL-97 [24]. Probable space groups based on systematic absences were $Cmc2_1$ (No. 36) and $Ama2$ (No. 40), both of which are noncentrosymmetric. The structure could only be solved and refined in the $Ama2$ space group. Pertinent crystallographic data and structure refinement details for $EuCu_2SnS_4$ are provided in Table 1. The atomic coordinates, equivalent displacement parameters and selected bond lengths and angles for $EuCu_2SnS_4$ are provided in Tables 2 and 3.

2.3.4. Differential thermal analysis (DTA)

DTA was performed using a Shimadzu DTA-50 thermal analyzer. DTA data were recorded using the TA60-WS collection program. The instrument was calibrated with a three-point calibration curve using the melting points of indium, zinc and gold metals. The temperature was programmed to increase at a rate of 10 °C/min from 25 to 1000 °C. The temperature then decreased to 100 °C at 10 °C/min. To determine reproducibility, a second cycle was performed in the same manner. The reference, Al_2O_3, and sample were contained in fused-silica ampoules (carbon coated for the sample) and sealed under a vacuum of $\sim 10^{-3}$ torr. Approximately 20 mg of sample and 20 mg of reference material were used for the measurement. The melting point was determined from the peak (minimum) of the endothermic event. The X-ray powder diffraction pattern of the DTA residue was collected and analyzed to determine if the material had decomposed or changed phase during thermal analysis.

2.3.5. Optical spectroscopy

An optical diffuse reflectance spectrum was obtained using a Varian Cary 5000 UV/Vis/NIR spectrometer. The sample was ground and loaded into a Harrick Praying Mantis diffuse reflectance accessory that uses elliptical mirrors. $BaSO_4$ was used as a 100% reflectance standard. Scans were performed from 2500 to 200 nm at a rate of 600 nm/min. Wavelength data were converted to electron volts and the percent reflectance data were converted to absorbance units using the Kubelka–Munk equation [25].

Table 1
Crystallographic data and structure refinement details for $EuCu_2SnS_4$

Empirical formula	$EuCu_2SnS_4$
Formula weight	525.97
Temperature	273(2) K
Wavelength	0.71073 Å
Space group	*Ama*2 (No. 40)
Unit cell dimensions	$a = 10.4793(1)$ Å
	$b = 10.3610(2)$ Å
	$c = 6.4015(1)$ Å
Volume	695.04(2) Å^3
Z	4
Calculated density	5.026 g/cm^3
Absorption coefficient	19.566 mm^{-1}
Crystal size	$0.17 \times 0.08 \times 0.05$ mm^3
Theta range for data collection	3.74 to 27.08°
Limiting indices	$-13 \leqslant h \leqslant 12$
	$-11 \leqslant k \leqslant 13$
	$-8 \leqslant l \leqslant 7$
Reflections collected	3369
Unique reflections	791 [R(int) = 0.0220]
Completeness to $2\theta = 27.08°$	100.0%
Max and Min transmission	0.4412 and 0.1357
Goodness-of-Fit on F^2	1.213
Final R indices [$I > 2\sigma(I)$]	$R1 = 0.99\%$ and $wR2 = 2.37\%$
Extinction coefficient	0.0068(1)
Absolute structure parameter	0.04(1)
Peak and hole (e/Å^3)	0.679 and −0.359

Table 2
Atomic coordinates and equivalent isotropic displacement parameters ($Å^2 \times 10^3$) for $EuCu_2SnS_4$

Atom	Site[a]	x	y	z	U (eq)[b]
Eu	4a	0	0	0.4803(1)	13(1)
Cu	8c	0.1256(1)	0.2898(1)	0.5649(1)	21(1)
Sn	4b	0.25	0.1496(1)	0.0600(1)	10(1)
S(1)	8c	0.0714(1)	0.2559(1)	0.2194(1)	12(1)
S(2)	4b	0.25	0.1014(1)	0.6967(2)	11(1)
S(3)	4b	0.25	0.4435(1)	0.7362(2)	11(1)

[a] The site is defined by Wycoff letter and multiplicity.
[b] U(eq) is defined as one third the trace of the orthogonalized U_{ij} tensor.

Table 3
Selected interatomic distances (Å) and angles (°) for $EuCu_2SnS_4$

Eu–S(1) 3.0497(8) × 2	
Eu–S(1) 3.2211(8) × 2	
Eu–S(2) 3.1444(6) × 2	
Eu–S(3) 3.1061(6) × 2	
Cu–S(1) 2.310(1), 2.3367(9)	S(1)–Cu–S(1) 99.04(2)
Cu–S(2) 2.494(1)	S(1)–Cu–S(2) 99.21(3), 109.46(3)
Cu–S(3) 2.3319(9)	S(1)–Cu–S(3) 115.66(3), 133.75(4)
	S(2)–Cu–S(3) 94.76(3)
Sn–S(1) 2.3996(7) × 2	S(1)–Sn–S(1) 102.56(4)
Sn–S(2) 2.378(1)	S(1)–Sn–S(2) 120.79(2) × 2
Sn–S(3) 2.415(1)	S(1)–Sn–S(3) 101.96(2) × 2
	S(2)–Sn–S(3) 105.73(4)
Cu–Cu 2.6077(8)	
Eu–Cu 3.228(4), 3.6803(5)	

3. Results and discussion

3.1. Synthesis and PXRD

$EuCu_2SnS_4$ was prepared from stoichiometric amounts of the constituent elements. Although several different heating conditions were tried, a phase-pure sample could not be prepared. PXRD of the product from the best synthesis in conjunction with Rietveld refinements allowed a determination of the composition of the product mixture. The results are shown in Fig. 1. The majority of the diffraction peaks can be indexed to the *Ama*2 structure of $EuCu_2SnS_4$ reported here. The Rietveld refinement gave 96.7 wt% for this major phase. Additional products were determined to be 2.8 wt% EuS (PDF# 03-065-5080) [26] and 1.6 wt% Cu_2SnS_3 (PDF# 01-089-2877) [27]. The diffraction pattern was examined carefully for the presence of peaks that could be attributed to the $P3_1$ structure of $EuCu_2SnS_4$ reported by Llanos [16]; however, they were absent from the pattern.

Despite the numerous synthetic conditions that we utilized under vacuum, we could never obtain the same results reported by Llanos and coworkers who used a CS_2/Ar stream. In addition to a difference of atmosphere, there also exists a difference in starting materials. It is important to note that while we started with high purity elements, Llanos and coworkers used EuS which was made via heating Eu_2O_3 under CS_2/Ar flow.

3.2. Structure

3.2.1. Structure description

$EuCu_2SnS_4$ possess the three-dimensional $SrCu_2GeSe_4$ structure-type [19], see Fig. 2. In this structure, each tin is bound to four sulfurs with a quite regular tetrahedral coordination; bond angles range from 101.96(2) to 120.80(2)°. The SnS_4 tetrahedra are isolated from one another and line up in rows along the *b* and *c* axes, see Fig. 3. They all point in the same direction along the *c* axis, rendering the structure noncentrosymmetric. The Sn–S bond distances are very regular with a range of 2.3789(12) –2.4150(11) Å. These compare well with the Sn–S distances in the related compounds. For example, 2.372(3)–2.409(3) Å for the related Sr_2SnS_4 [12] or 2.38–2.40 Å for $SrCu_2SnS_4$ [17].

The copper atoms are also tetrahedrally coordinated by sulfur, but are much more irregular than the SnS_4 tetrahedra discussed above. The CuS_4 tetrahedra alone form layers in the *ac* plane. Each tetrahedron is connected to three others by sharing an edge with one other tetrahedron and two of its corners with two other

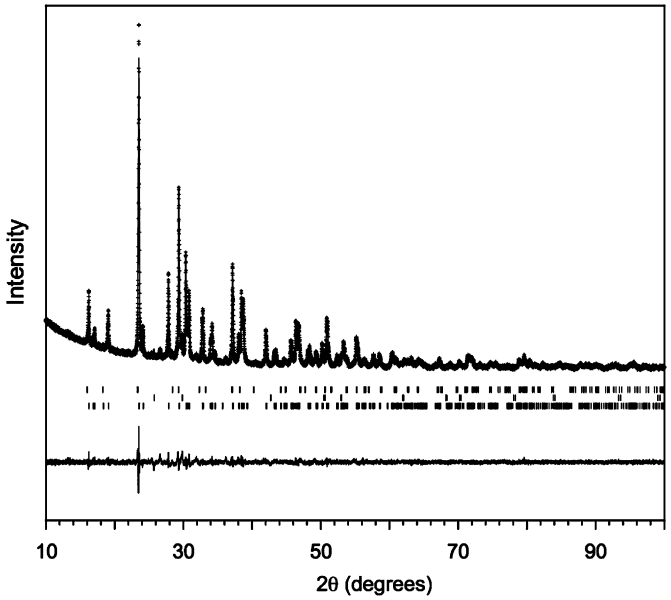

Fig. 1. Rietveld refinement of the three-phase mixture containing 96.7 wt% $EuCu_2SnS_4$, 2.8 wt% EuS and 1.6 wt% Cu_2SnS_3 ($R_{wp} = 2.83\%$, $R_p = 2.06\%$, $\chi^2 = 1.467$). Observed (+++) and calculated (solid line) X-ray diffraction patterns for the three-phase mixture are shown on top. The difference between observed and calculated intensities is shown as a difference plot on the bottom. Three sets of tick marks in between indicate allowed Bragg reflections for Cu_2SnS_3, EuS and $EuCu_2SnS_4$, from top to bottom, respectively.

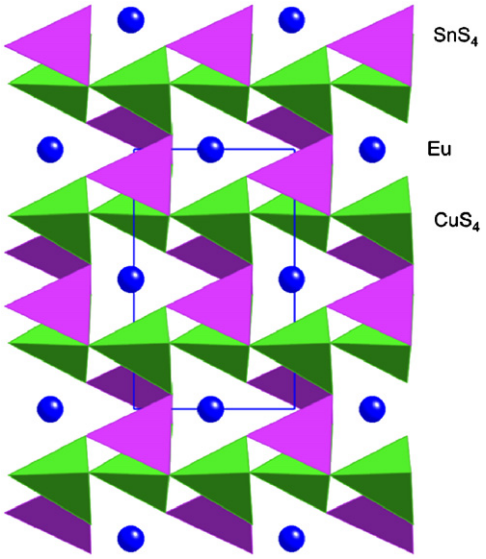

Fig. 2. $EuCu_2SnS_4$ viewed down the crystallographic *a* axis.

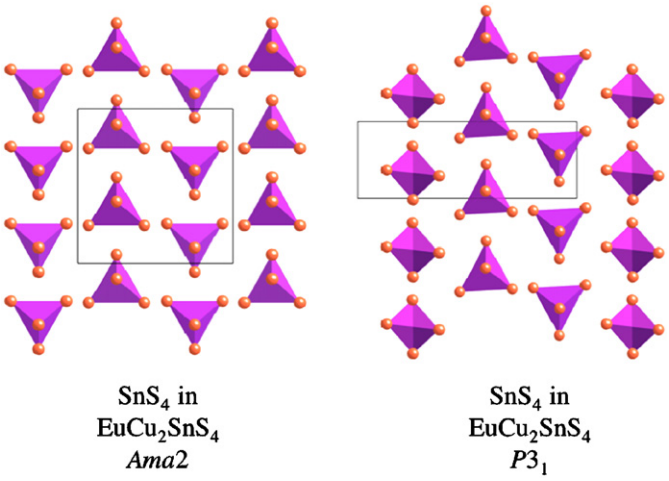

Fig. 3. SnS_4 tetrahedra in $EuCu_2SnS_4$. The arrangement on the left comes from the *Ama*2 structure viewed down the *c* axis, while the arrangement on the right is found in the $P3_1$ structure viewed down the *a* axis. These corresponding axes are approximately 6.3–6.4 Å.

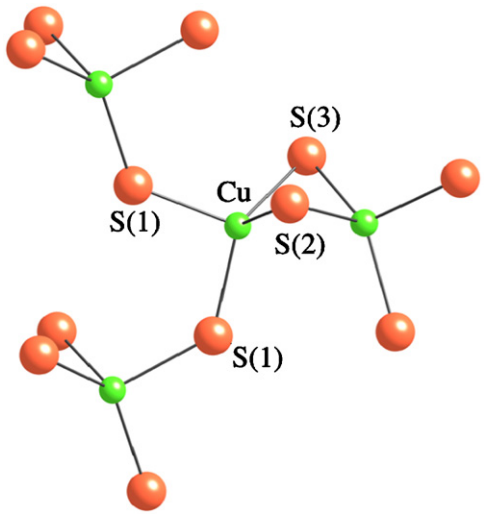

Fig. 4. Extended coordination sphere of copper in $EuCu_2SnS_4$, showing how each CuS_4 unit connects to three others using one edge and two corners.

tetrahedra, see Fig. 4. The CuS_4 tetrahedra are also pointing in the same direction along the *c* axis, thus contributing to the noncentrosymmetric nature of the structure. Combining the CuS_4 layers with the isolated SnS_4 creates a three-dimensional network in which each SnS_4 connects to eight CuS_4 by using all four of its corners, see Fig. 2. Cu–S bond distances range from 2.3106(10) to 2.4941(10)Å; tetrahedral angles range from 99.04(2) to 133.75(4)°. These Cu–S bond distances are rather typical and compare well with those found in $SrCu_2GeS_4$, 2.32–2.49 Å [18].

There is a relatively short Cu–Cu distance of 2.6077(8)Å between copper atoms of the tetrahedra that share edges. This short Cu–Cu distance compares well with that found in the isostructural $BaCu_2SnSe_4$ (2.7030(14)Å) and $SrCu_2GeS_4$ (2.622(6)Å) [19,20]. Electronic structure calculations indicate that such close Cu–Cu distances result in an overall bonding interaction, yet have very little contribution near the Fermi level and little impact on the band gap of the resulting materials [20].

Each europium cation is coordinated to eight sulfurs forming a square antiprism. The EuS_8 polyhedra use all sulfurs to connect to six other EuS_8 units, two via edges along the *a* axis and four via corners along the *b* and *c* axes. Therefore the EuS_8 alone form a

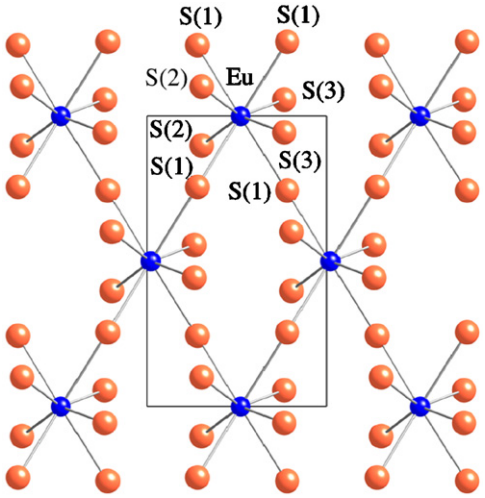

Fig. 5. Europium–sulfur, three-dimensional framework in $EuCu_2SnS_4$ viewed down the crystallographic *a* axis.

3-dimensional network, see Fig. 5. Alternatively one can think of the $[Cu_2SnS_4]^{2-}$ framework as creating tunnels that run down the *a* axis where the Eu^{2+} cations align themselves in rows, see Fig. 2. The Eu–S distances are very regular and fall within the narrow range of 3.0497(8)–3.2211(8)Å. Eu-S distances in other compounds with eight-coordinate $Eu^{2+}S_8$ units are similar, for example in 2.989(2)–3.303(3)Å in $Eu_3Sn_2S_7$ [10] and 2.954(1)–3.101(1)Å in Eu_2SnS_4 [12].

3.2.2. Structure comparison

Based on PXRD data, Llanos and coworkers reported a different structure for $EuCu_2SnS_4$ [16]. They reported that the compound crystallizes in the space group $P3_1$, specifically the $SrCu_2SnS_4$ structure-type [17]. Later Kolis and coworkers [28] proposed that the space group for $SrCu_2SnS_4$, $SrCu_2GeS_4$ and $BaCu_2GeS_4$ may actually be $P3_221$ based on infrared data compared with the isostructural $RbAg_2SbS_4$. In the $P3_1$ (or $P3_221$) structure each CuS_4 tetrahedron corner shares with four others, creating a three-dimensional network. This differs from the *Ama*2 structure where the CuS_4 units form layers. In the $P3_1$ structure Eu cations form square antiprisms that are much more distorted compared to the EuS_8 in the *Ama*2 structure. In the $P3_1$ (or $P3_221$) structure, these "square antiprisms" connect to eight others by sharing only corners, while in the *Ama*2 structure the square antiprisms connect by sharing both corners and edges. Another important difference between the two structures is that although the SnS_4 tetrahedra are isolated in both structures, they do not pack together in the same way, see Fig. 3.

The fact that the structure reported here does not agree with that published by Llanos and coworkers [16] is intriguing. Considering that the ionic radius of Sr^{2+} is less than 1% larger than that of Eu^{2+} [29] it is not surprising that Llanos and coworkers found $EuCu_2SnS_4$ to crystallize in the same structure as the strontium analog [19]. However, what seems like a discrepancy may not be, as different preparation conditions certainly can, and have been known to, create compounds with the same chemical formula but different structure types (polymorphs). As a highly related example, one can consider the structure of Sr_2SnS_4. This compound was reported by Flauhart and coworkers [11] to crystallize in the *Pnma* space group, as does Eu_2SnS_4. However, Johrendt and coworkers [12] later found Sr_2SnS_4 to crystallize in the *Ama*2 space group. Likewise, Johrendt et al. proposed that the difference in synthetic conditions may have lead to the different structures obtained.

Obviously, there must be a small energy difference between the two structures, in the case of Sr_2SnS_4 (*Pnma* vs. *Ama*2) and $EuCu_2SnS_4$ ($P3_1$ vs. *Ama*2). Also, it was suggested by Johrendt et al. [12] that an important factor that determines the structure in these systems is the balance between tetrahedral packing, which is ideally as close as possible, and the optimal coordination sphere of the larger cation within this packing arrangement. This balance can probably be tipped in either direction in certain systems, such as the one reported here.

An examination of the literature found several compounds, chemically related to the title compound, possessing the same $SrCu_2GeSe_4$ structure-type with space group *Ama*2. Additionally, several other chemically related compounds have similar structures, see Table 4. An important feature of these structures is the identical packing of near-perfect tetrahedra: SnS_4, $SnSe_4$, $GeSe_4$ or PSe_4. Within this packing arrangement, small holes can accommodate four-coordinate cations such as Li^+ or Cu^+, which adopt distorted tetrahedral coordination. Alternatively, in the case of Sr_2SnS_4 and γ-Sr_2GeSe_4 these holes can remain void. Additionally, eight-coordinate cations, such as Sr, Ba or Eu, may reside in the larger holes created by this packing arrangement.

3.3. Physical property measurements

3.3.1. Optical diffuse reflectance spectroscopy

The optical diffuse reflectance spectrum for a powdered sample of $EuCu_2SnS_4$ shows the compound to be a semiconductor with a band gap of 1.85 eV, see Fig. 6. This is consistent with the dark red color of the material.

Table 4
Comparison of related compounds, A_2CD_4, AB_2CD_4 and $ABCD_4$, crystallizing in the *Ama*2 space group

Formula	A site(s)	B site	C site	D sites	Reference
Sr_2SnS_4	4a, 4b		4b	4b, 4b, 8c	[12]
γ-Sr_2GeSe_4	4a, 4b		4b	4b, 4b, 8c	[12]
$BaCu_2SnSe_4$	4a	8c	4b	4b, 4b, 8c	[20]
$SrCu_2GeSe_4$	4a	8c	4b	4b, 4b, 8c	[19]
$EuCu_2SnS_4$	4a	8c	4b	4b, 4b, 8c	This work
$LiEuPSe_4$	4a	4a	4b	4b, 4b, 8c	[8]

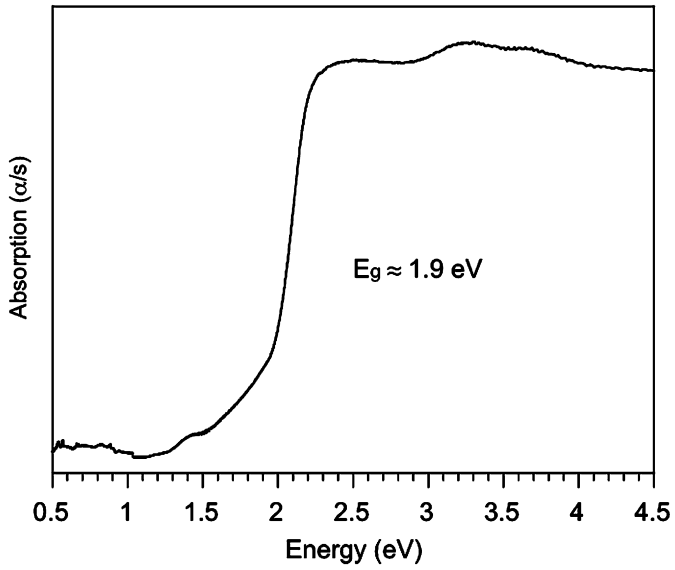

Fig. 6. Optical diffuse reflectance spectrum converted to absorption for a powdered sample of $EuCu_2SnS_4$.

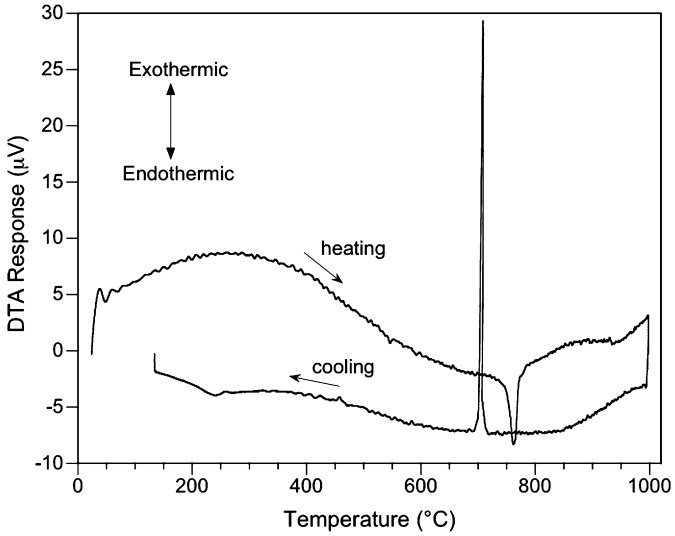

Fig. 7. Differential thermal analysis diagram obtained for $EuCu_2SnS_4$.

3.3.2. Differential thermal analysis (DTA)

The DTA diagram obtained for $EuCu_2SnS_4$ shows a melting point at approximately 762 °C and a corresponding recrystallization at 709 °C, see Fig. 7. There are several small, additional features in the diagram that may be due to the impurity phases present before thermal analysis and/or a result of partial decomposition or additional phases resulting from side-reactions with the fused-silica ampoule during thermal analysis. PXRD of the DTA residue suggests that the compound has partially decomposed during thermal analysis, as the majority of the diffraction peaks can still be attributed to $EuCu_2SnS_4$ (*Ama*2), but the impurity peaks for Cu_2SnS_3 have increased in intensity. However, careful analysis also indicates the presence of an oxysulfide phase, Eu_2O_2S (PDF#03-065-3450) [30], as a result of a reaction with the ampoule despite careful carbon coating.

4. Conclusion

$EuCu_2SnS_4$ has been synthesized and found to adopt the $SrCu_2GeSe_4$ structure-type. In this structure, Eu^{2+} is found to adopt a square anti-prismatic coordination, thus mimicking similar alkaline-earth-containing phases. Due to the noncentrosymmetric nature of the structure, this material may be useful for second harmonic generation.

Supporting Information

Further details of the crystal structure investigation may be obtained from Fachinformationszentrum Karlsruhe, 76344 Eggenstein-Leopoldshafen, Germany (Fax: +49 7247 808 666; e-mail: crysdata@fiz-karlsruhe.de, http://www.fiz-karlsruhe.de/request_for_deposited_data.html). CSD number X.

Acknowledgments

Support from J.A. Aitken's National Science Foundation Career Award (DMR-06-45304) is gratefully acknowledged. The Bruker Apex II CCD and the PANalytical X'Pert Pro MPD X-ray diffractometers were purchased with funds from the National Science Foundation (CRIF 02-34872 and DUE 05-11444). The Varian Cary 5000 and Shimadzu DTA50 were purchased with start-up funds

provided by the Bayer School of Natural and Environmental Sciences at Duquesne University.

Appendix A. Supplementary data

Supplementary data associated with this article can be found in the online version at doi:10.1016/j.jssc.2008.09.022.

References

[1] T. Jiang, G.A. Ozin, J. Mater. Chem. 8 (1998) 1099–1108.
[2] M. Tampier, D. Johrendt, J. Solid State Chem. 158 (2001) 343–348.
[3] T.L. Volkonskaya, A.G. Gorobets, S.A. Kizhaev, I.A. Smirnov, V.V. Tikhonov, M. Guittard, C. Lavenant, J. Flahaut, Phys. Status Solidi A 57 (1980) 731–734.
[4] J.A. Aitken, J.A. Cowen, M.G. Kanatzidis, Chem. Mater. 10 (1998) 3928–3935.
[5] J.A. Cowen, P. Michlin, J. Kraus, S.D. Mahanti, J.A. Aitken, M.G. Kanatzidis, J. Appl. Phys. 85 (1999) 5381–5383.
[6] W. Bensch, P. Durichen, Chem. Ber. Recl. 129 (1996) 1489–1492.
[7] C.R. Evenson IV, P.K. Dorhout, Inorg. Chem. 40 (2001) 2049–2414.
[8] J.A. Aitken, K. Chondroudis, V.G. Young Jr., M.G. Kanatzidis, Inorg. Chem. 39 (2000) 1525–1533.
[9] A. Choudhury, L.A. Polyakova, S. Strobel, P.K. Dorhout, J. Solid State Chem. 180 (2007) 1381–1389.
[10] S. Jaulmes, M. Julien-Pouzol, Acta Cryst. B 33 (1977) 3898–3901.
[11] J. Flahaut, P. Laruelle, M. Guittard, S. Jaulmes, M. Julien-Pouzol, C. Lavenant, J. Solid State Chem. 29 (1979) 125–136.
[12] R. Pocha, M. Tampier, R.-D. Hoffmann, B.D. Mosel, R. Pottgen, D. Johrendt, Z. Anorg. Allg. Chem. 629 (2003) 1379–1384.
[13] G. Bugli, D. Carre, S. Barnier, Acta Cryst. B 34 (1978) 3186–3189.
[14] S. Jaulmes, M. Julien-Pouzol, Acta Cryst. B 33 (1977) 1191–1193.
[15] P. Jakubcova, D. Johrendt, C.P. Sebastian, S. Rayaprol, R. Pottgen, Z. Naturforsch. B 62 (2007) 5–14.
[16] J. Llanos, C. Mujica, V. Sánchez, Octavio, Peña, J. Solid State Chem. 173 (2003) 78–82.
[17] C.L. Teske, Z. Anorg. Allg. Chem. 419 (1976) 67–76.
[18] C.K. Teske, Z. Naturforsch. 34b (1979) 386–389.
[19] M. Tampier, D. Johrendt, Z. Anorg. Allg. Chem. 627 (2001) 312–320.
[20] A. Assoud, N. Soheilnia, H. Kleinke, J. Solid State Chem. 17 (2005) 2255–2261.
[21] A.C. Larson, R.B. Von Dreele, General Structure Analysis System (GSAS) Los Alamos National Laboratory Report LAUR 86-748, 1994.
[22] B.H. Toby, J. Appl. Crystallogr. 34 (2001) 210–213.
[23] SAINT and SADABS are Part of the Apex 2 Software Package v2.1-4 Program for Data Collection and Reduction on Bruker AXS CCD Area Detector Systems, Bruker Analytical X-Ray Systems, Inc., Madison, WI, 2005.
[24] G.M. Sheldrick, Acta Cryst. A 64 (2008) 112–122.
[25] P. Kubelka, F. Munk, Z. Tech. Phys. Tr. Stephen H. Westin 12 (1931) 593–601.
[26] K. Westerholt, H. Endrikat, R. Dahlbeck, H. Bach, J.P. Sanchez, J.M. Friedt, Phys. Rev. B 33 (1986) 567–577.
[27] L.S. Palatnik, Y.F. Komnik, E.K. Belova, L.V. Adroschenko, Dokl. Akad. Nauk. SSSR 137 (1961) 68–71.
[28] G.L. Schimek, W.T. Pennington, P.T. Wood, J.W. Kolis, J. Solid State Chem. 123 (1996) 277–284.
[29] R.D. Shannon, Acta Cryst. A 32 (1976) 751–767.
[30] H.A. Eick, J. Am. Chem. Soc. 80 (1958) 43–44.